JOURNAL OF GEOPHYSICAL RESEARCH, VOL. 103, NO. A12, PAGES 29,253–29,266, DECEMBER 1, 1998

Ionospheric structure and the generation of auroral roar

S. G. Shepherd and J. LaBelle

Department of Physics and Astronomy, Dartmouth College, Hanover, New Hampshire

R. A. Doe and M. McCready

Radio Science and Engineering Division, SRI International, Menlo Park, California

A. T. Weatherwax

Institute for Physical Science and Technology, University of Maryland, College Park

Abstract. Ionospheric electron density data from the Sondrestrom incoherent scatter radar (ISR) have been used to characterize the structure of the F region ionosphere during ground-based LF/MF/HF receiver observations of natural ionospheric radio emissions known as auroral roar. In five out of six cases, the F region ionosphere has significant horizontal N_e gradient scale lengths ($|\nabla N_e/N_e|^{-1}_{min} < 120$ km, measured with 23–137 km spatial resolution). In three of these cases, localized F region auroral ionospheric cavities, with horizontal scales ~50 km, are observed. In one of six cases, the ionosphere lacks either of these features, and a laminar, mostly unstructured, F region is observed. The data suggest that auroral roar events may occur for a range of large-scale (>30 km) ionospheric conditions. Some theories for the generation of auroral roar require that the relationship between the electron plasma frequency (f_{pe}) and the electron gyrofrequency (f_{ce}) in the source region is $f_{pe}^2 = (n^2 - 1)f_{ce}^2$, where n is the harmonic number of the observed emission. Comparisons between observed auroral roar emission frequencies, ISR observations of electron density, and the IGRF model for the magnetic field show that this frequency-matching condition holds somewhere in the ionosphere in 16 out of 18 cases studied and in all 3 cases of ISR elevation scans capable of measuring a source located directly overhead.

1. Introduction

Auroral roar is a relatively narrow-band radio-wave emission ($\delta f/f < 0.1$) generated in the auroral ionosphere at frequencies near 2 and 3 times the electron cyclotron frequency (f_{ce}) [*Kellogg and Monson*, 1979, 1984; *Weatherwax et al.*, 1993, 1995]. Recent evidence strongly suggests that the $2f_{ce}$ emissions originate where the wave frequency f matches $2f_{ce}$ in the F region of the ionosphere [*Hughes and LaBelle*, 1998]. Seasonal, diurnal, and spectral characteristics of auroral roar have been documented [*LaBelle and Weatherwax*, 1992; *Weatherwax et al.*, 1993, 1995; *Weatherwax*, 1994; *LaBelle et al.*, 1995; *Shepherd et al.*, 1998; *Hughes and LaBelle*, 1998], and several theories of generation mechanisms have been presented [*Weatherwax*, 1994; *Weatherwax et al.*, 1995; *Yoon et al.*, 1996, 1998a; *Willes et al.*, 1998]. Simultaneous measurement of ionospheric structure provides a test of such generation mechanisms, yet no electron density measurements have previously been reported during auroral roar observations. An earlier attempt using ionosonde data in Alaska proved unfruitful because the ionograms were too disturbed at times of auroral emissions [*Weatherwax*, 1994, p. 48].

Several theories of auroral roar generation require the presence of localized F region electron density cavities of the type first described by *Doe et al.* [1993] to provide regions for enhanced wave growth resulting from reflections at the cavity boundaries, to allow wave mode conversion on the density gradients of the cavity or from coalescence of reflecting waves [*Yoon et al.*, 1998; *Willes et al.*, 1998], and to provide for ducting of O or X mode waves to the ground [*Yoon et al.*, 1996]. The presence or absence of these N_e cavity structures during roar observations can be determined with the electron density measurements from the ISR. Other theories predict that auroral emissions occur when the upper hybrid frequency (defined by $f_{uh}^2 = f_{ce}^2 + f_{pe}^2$) is equal to a harmonic of the electron cyclotron frequency (f_{ce}) [e.g., *Kaufmann*, 1980; *Gough and Urban*, 1983; *Weatherwax et al.*, 1995]. Using ISR density measurements, this up-

Paper number 98JA02295.
0148-0227/98/98JA-02295$09.00

per hybrid matching condition can be tested in the F region of the ionosphere during observations of auroral roar. The ISR electron density measurements provide the opportunity to determine whether these theories can still be considered viable candidates for explaining auroral roar.

In 1995, Dartmouth researchers installed a programmable stepped frequency receiver (PSFR) at the Sondrestrom radar facility (66.987° N latitude, 309.051° E longitude, 73.3 invariant). By operating the PSFR on a continuous basis, we achieved significant overlap with ongoing ISR operations. A number of coincidences did occur during auroral roar events and are analyzed in the following sections. Section 2 presents the data for these periods, and sections 2.1 and 2.2 address ionospheric structure features and the upper hybrid matching condition, respectively.

2. Data Presentation

The PSFR, described in detail elsewhere [e.g., *Weatherwax*, 1994], operates in a standard mode which sweeps each 2 s from 30 kHz to 5 MHz with 10-kHz resolution and operates for 20 hours each day centered on local midnight. The PSFR has a dynamic range of ~70 dB and an instrument sensitivity of a few nV m^{-1} $Hz^{-1/2}$, though in practice the noise floor at the Sondrestrom site is significantly higher than this level. The non resonant dipole antenna used in this system is sensitive to electromagnetic wave fluctuations emanating from a large portion of the sky; for example, the antenna sensitivity to a radio wave propagating from an azimuthal angle of 45° (~300 km ground range) is at worst half that compared to a wave propagating from directly overhead. Radio wave observations from ground stations located in Canada and separated by ~275 km suggest that auroral roar often originate from nearly overhead.

Kelly et al. [1995] present a recent description of the capabilities of the Sondrestrom radar and ancillary ground–based instruments. During the auroral roar observations presented below, the Sondrestrom ISR operated in one of three modes, performing elevation or composite scans and providing several degrees of latitudinal coverage of plasma parameters. The horizontal resolution of each experiment mode will be discussed later. The transmitter pulse length for these experiments was 320 μs, and thus autocorrelation functions were formed with a range resolution of 48 km.

To identify study intervals, the survey spectrograms of the PSFR data were first systematically searched for occurrences of auroral roar. By comparing these occurrences with the radar operation schedule, a subset of these events was identified for which the ISR was in an appropriate mode to measure the two-dimensional electron density distribution in the F region ionosphere. Six such days including 18 individual radar scans are the focus of this study. The small number of coincidences during 1995 to 1997 is in part due to radio frequency interference from equipment in the radar facility which obscures many auroral radio emissions. The PSFR antenna has recently been moved further away from noise sources, an improvement which should increase opportunities for joint PSFR/ISR observations during future auroral roar observations.

2.1. Ionospheric Structure

PSFR and ISR scans for the six selected observation days are presented in Plates 1 through 6. At the top of each Plate the PSFR data is displayed as a grayscale image. The gray level corresponds to the intensity of the received signal with darker pixels representing stronger signals and a roughly 35 dB difference between black and white pixels. The horizontal axis is universal time (UT) and the vertical axis is frequency. Midnight magnetic local time corresponds to 0217 UT at ground level. Both the time and frequency scales vary between plates. Horizontal dark lines in the grayscale are fixed-frequency anthropogenic transmissions such as short-wave radio, AM band, and navigational transmissions.

Vertical black lines superposed on the grayscale plots indicate the start and stop times of ISR scans. The electron density profiles measured during these scans are shown below the grayscale plots as false color plots. Electron densities for which the estimated error is less than 50% are shown, but the uncertainty, which depends primarily on the density, is typically less than 10% at F region altitudes. Letters (A, B, C, etc.) indicate which color density plot corresponds to which period in the grayscale plot. All electron density color plots have been rendered on grids with identical scales: the vertical axis is altitude 75–500 km, the horizontal axis is ground range (magnetic north) from the facility, −500–500 km, and the color bar displays the logarithm of the electron density from 1.0×10^4 cm^{-3} to 3.2×10^5 cm^{-3}. In Plate 4, all the ISR scans are elevation scans (through the zenith) which are rendered on meridional grids. In all other plates (1, 2, 3, 5, 6), composite (mixed elevation/azimuth) scans were conducted, in which alternating scan planes are offset to the east and west in a manner described by *Weber et al.* [1991]. In these cases, each composite scan has been geometrically projected onto the meridional plane. A small curved arrow near the origin of the contour plot indicates the direction of the scan. The vertical geometric projection of the azimuthal angle of the radar beam is shown in the lower left corner of each panel with the progression of the scan indicated by colors ranging from green (start of scan) to red (end of scan).

Plate 1 shows an example of both $2f_{ce}$ and $3f_{ce}$ auroral roar events observed on August 3, 1995. Observations of $3f_{ce}$ roar, first reported by *Weatherwax et al.* [1993], are much less common than $2f_{ce}$roar. Segments B and C of the grayscale show the $3f_{ce}$ roar event starting at 0110 UT near 4 MHz. In the middle of segment C a radio emission can be seen at a slightly lower fre-

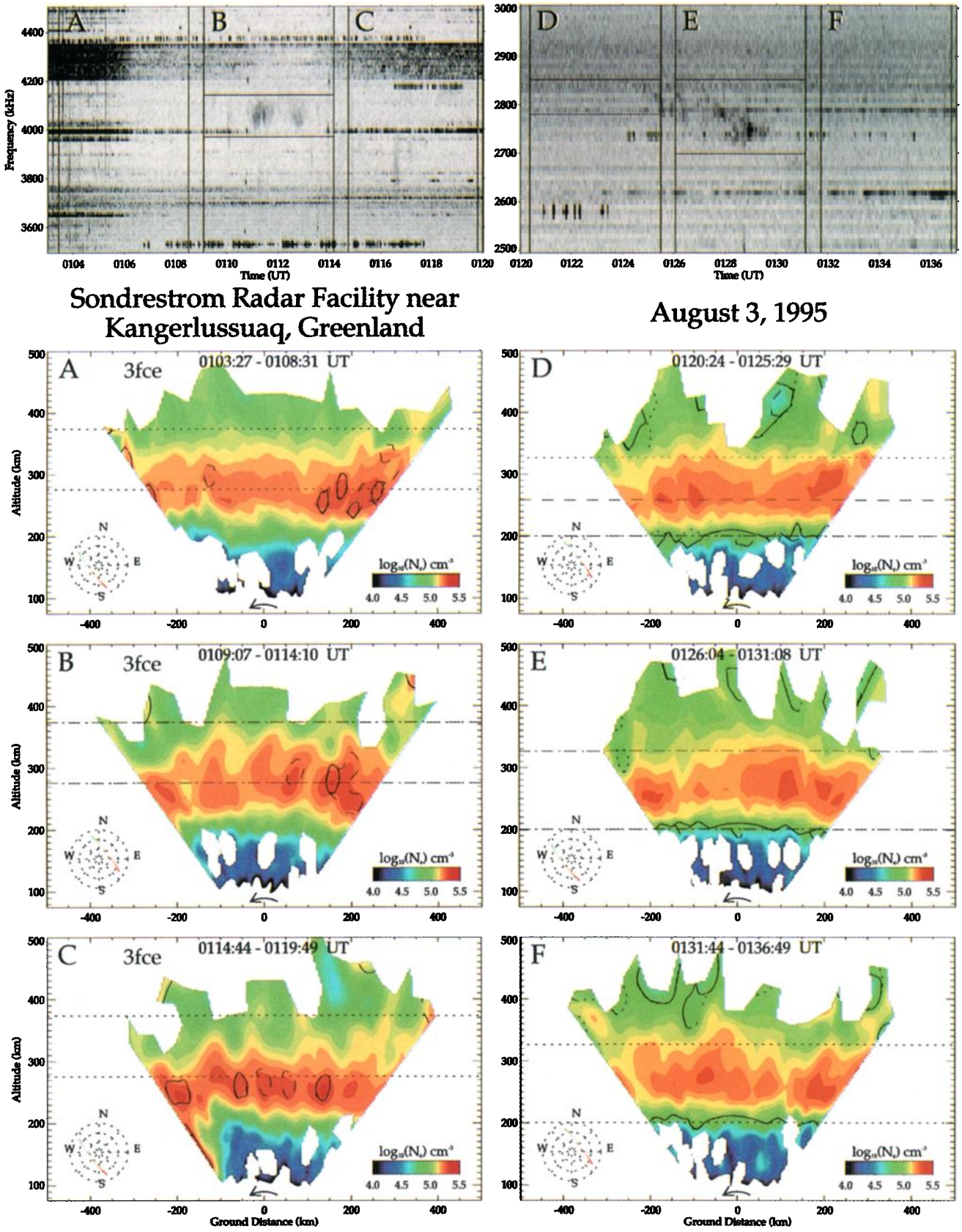

Plate 1. August 3, 1995, auroral roar event is shown with a PSFR grayscale plot and accompanying pseudo color density plot from the ISR. See text for details on dynamic range and spatial scales. This example shows the F region ionosphere to be mostly laminar during the observation of $2f_{ce}$ and $3f_{ce}$ auroral roar emissions.

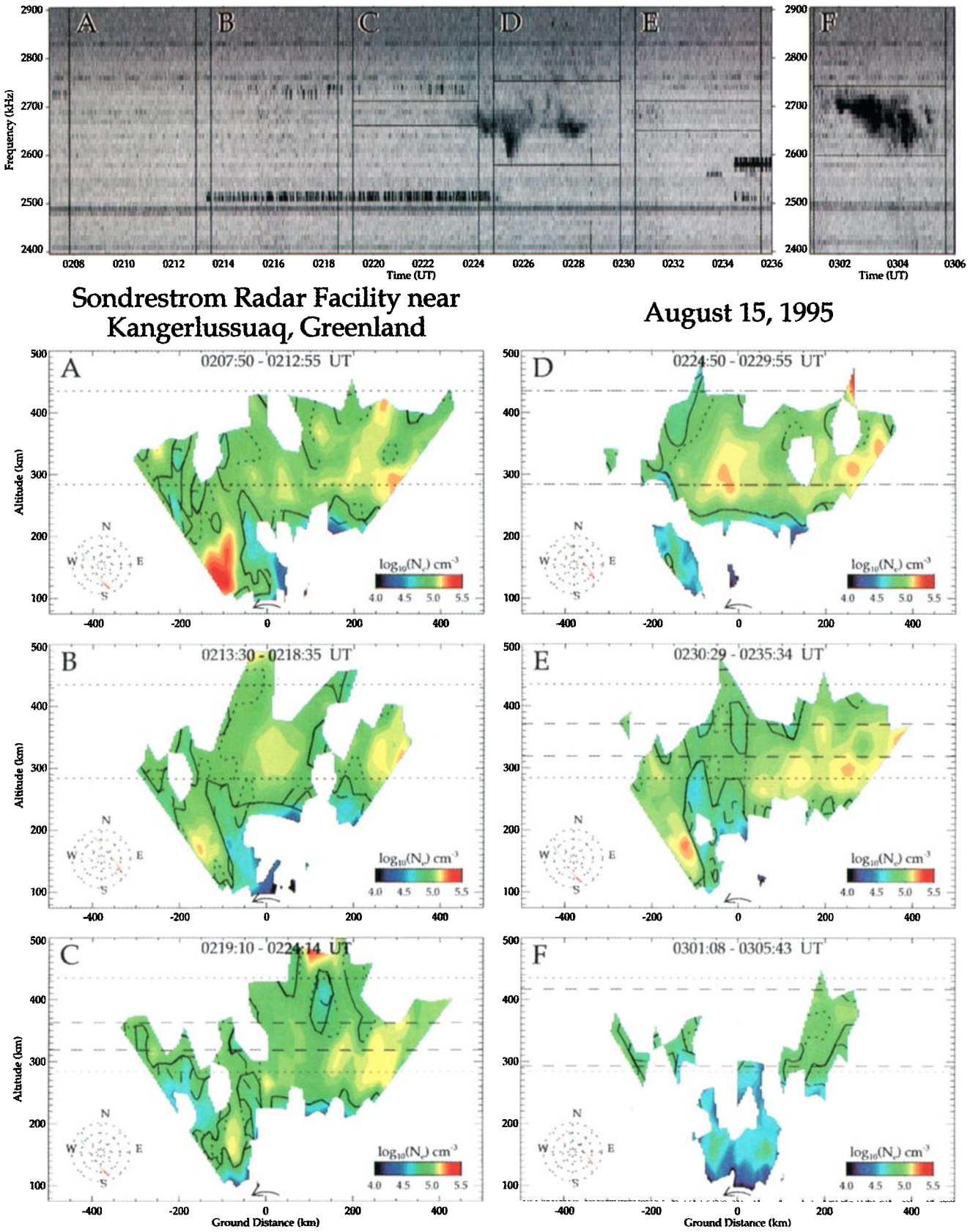

Plate 2. August 15, 1995, auroral roar event. An example showing an E region arc, corresponding auroral ionospheric cavity, strong N_e gradients, and adequate upper hybrid matching.

quency, but this probably represents a different type of emission called an MF Burst [*Weatherwax et al.*, 1994; *LaBelle et al.*, 1997]. Segments D and E show a related, but uncorrelated, $2f_{ce}$ roar emission near 2.8 MHz starting around 0125 UT and present during nearly all of segment E. For this experiment, the ISR performed composite scans (moving in both azimuth and elevation) such that planes parallel to the magnetic meridian, but offset by 20° to the east and again to the west, are probed. The scan rate varied, by design, to give constant ground tracking. The processed data integration of 15 s results in a horizontal spatial resolution at 275 km altitude of 23 km.

The corresponding ISR scans show the F region ionosphere (H_{max} = 270 km, $N_e^{max} = 1.96\times10^5$ cm^{-3}) during these two events to be mostly laminar without significant electron density structure ($|\nabla N_e/N_e|^{-1}_{min} > 200$ km). Discrete, weak E layer arcs, signified by patches of enhanced plasma density between 100 and 200 km due to increased ionization from energetic auroral electrons in the upward current region are observed throughout this period. An E region arc appears at the equatorward edge of scan C, but the F region ionosphere north of the arc is notably smooth. No significant horizontal gradients are observed, and there are no auroral ionospheric cavities, discussed by *Doe et al.* [1993], observed during this event (such cavities would be visible as a region of low plasma density extending through the F region due to evacuation in the downward current region).

Plate 2 shows a particularly intense $2f_{ce}$ auroral roar event observed on August 15, 1995, beginning around 0222 UT, toward the end of scan C. The emission is particularly strong during radar scan D and trails off during the following scan. After an interlude of nearly 28 min with no roar observations, another strong emission is observed starting at 0301 UT (segment F). The ISR operating mode was identical to that of the first experiment, and the resulting resolution is the same as that of Plate 1.

The series of ISR scans for this event indicate that the field of view is at the edge of the polar cap boundary with an E region boundary arc, an auroral ionospheric cavity, and a structured F region ionosphere. Significant horizontal ionization gradients are observed in the polar cap north of the arc. For example, the density of the F region at H_{max} = 270 km varies from $N_e = 1.06\times10^5$ cm^{-3} (f_{pe} = 2.92 MHz) in the middle of an ionization patch to $N_e = 4.32\times10^4$ cm^{-3} (f_{pe} = 1.87 MHz) in the middle of a cavity over a scale length of approximately 60 km. The ionospheric cavity begins to form slightly equatorward of the radar in scan C and is apparent in scans D and E. The composite scans provide an estimate of the zonal extent of the ionospheric cavity (~250 km) and its duration (~20 min). Scan F, corresponding to the second strong roar, also suggests significant horizontal F region gradients.

Plate 3 shows an example of $2f_{ce}$ roar observed on November 1, 1995, beginning near 1927 UT and continuing intermittently for nearly 30 min. During this time the center frequency of the roar rises from ~2.65 MHz to ~2.75 MHz. The ISR operating mode was identical to that of the first two experiments, and the resulting resolution is the same as that of Plates 1 and 2.

This period is characterized by the intermittent observation of a strong E region arc (1938–1959 UT) and significant F region horizontal gradients to the north. A shallow depletion is observed immediately poleward of the arc in scan C. This feature mimics the morphology of a typical auroral ionospheric cavity but cannot be unambiguously classified without prior observation of the characteristic ambient F region electron density, which is difficult to determine due to the intrinsic 'patchiness' during this period. During scan B, just prior to panel C, there appears to be a depletion in the F region with minimum density at the core of this depleted region on the order of $N_e = 6.2\times10^4$ cm^{-3} (f_{pe} = 2.23 MHz), ~55% below N_e^{max}. It is unlikely that the depletion shown in panel B is related to a downward field-aligned current filament, the classic auroral ionospheric cavity formation agent, as there is little evidence for an associated upward field-aligned current signature such as an E region arc. This density depletion may be, however, a fossil cavity which has advected into the ISR field of view. Depletions of this scale were observed continuously from 1907 through 1935 UT (not shown).

Plate 4 shows a $2f_{ce}$ auroral roar event observed on March 12, 1996, beginning near 0057 UT, weakening for ~15 min, and returning in an intense burst near 0116 UT. During this event, the ISR was performing a series of elevation scans through the zenith, covering more latitude than in the earlier experiments. These scans were done at a constant angular rate (giving variable ground tracking). The horizontal spatial resolution at 275 km altitude varied from 137 km at the ends of the scans to 44 km when the scan went overhead. For these scans, most of the interesting ionospheric structure lies within 45° of zenith, a region with an average horizontal spatial resolution at 275 km altitude of 60 km.

An auroral ionospheric cavity was observed to form in ISR scans C and D, and it can be observed during two subsequent scans E and F. Scan C (starting at 0104:33 UT) shows a classic cavity with an F region depleted by 45% to a value of $N_e = 5.62\times10^4$ cm^{-3} (f_{pe} = 2.13 MHz). Prior to 0104:33 UT the E region arc is too far south of the radar to adequately bound the equatorward edge of the ionospheric cavity, but the depleted F region to the south of zenith is most likely coincident with the cavity. The F region ionosphere is patchy during this entire period, and the scans include the boundary of the auroral zone/polar cap, similar to the scenario for August 15, 1995 (Plate 2).

Plate 5 shows a $2f_{ce}$ auroral roar event observed on March 29, 1996, near 2.7 MHz starting near 2340 UT

(scan C) in the presence of severe radio frequency interference. A separate emission, called MF-burst, can also be seen during this time at a lower frequency (~2.5 MHz). The ISR operating mode was identical to that of the first three experiments, and the resulting resolution is the same as that of Plates 1, 2, and 3. The sequence of ISR scans from panel B to panel E has similar salient features as described for the August 15, 1995, and the March 12, 1996, events (Plates 2 and 4): a well-structured polar cap F region ionosphere, a dense E region auroral arc, and an F region auroral ionospheric cavity between them. The latitudinal extent of the cavity appears to grow somewhat larger (~120 km) in scan C, but it tracks the poleward boundary of the aurora in all six scans. For the scan associated with the auroral roar emissions (panel C), the F region is depleted by approximately 65% to a value of $N_e = 4.48 \times 10^4$ cm^{-3} ($f_{pe} = 1.55$ MHz).

Plate 6 shows a $2f_{ce}$ auroral roar event observed on April 9, 1997, starting near 0015 UT and occurring intermittently through radar scans labeled A-F. The ISR mode was similar to that of Plate 1 (constant ground tracking composite scans), but the radar covered more latitude and scanned at an overall faster rate, and the scans were offset to the east and west by 25°. The resulting horizontal spatial resolution at 275 km altitude is 36 km. The absolute electron density in the F region overhead is higher than in most of the examples shown here, with the exception of the August 3 event (Plate 1), which this event resembles in the respect. However, unlike the August 3 event, significant horizontal F region gradients are present and persist during all of the ISR scans. For instance, several regions are evident where the density is depleted by ~55% to a minimum value of $N_e = 5.75 \times 10^4$ cm^{-3} ($f_{pe} = 2.15$ MHz). No E region arc is evident in these scans and hence no ionospheric cavity. There is evidence for a broad dip in the electron density to the south which persists for over 20 min during scans A through F.

The 6 days of auroral roar observations shown in this paper are characterized by a variety of ionospheric conditions summarized in Table 1. Five out of six auroral roar events can be related to a depleted F region ionosphere, characterized by patchiness and relatively large horizontal density gradients or relatively small gradient scale lengths ($|\nabla N_e/N_e|^{-1}_{min} < 120$ km measured with 23–137 km resolution), and three of these are associated with classic auroral ionospheric cavities at the poleward edge of the auroral zone. The remaining event occurs when the F region ionosphere is unstructured and laminar.

The existing theories of auroral roar generation can be classified as either direct or indirect depending on whether electromagnetic (EM) radiation is stimulated in the source region and propagates directly to the ground in the O or X mode, or electrostatic (ES) Z mode waves are generated and mode convert to an escaping O or X mode. Several of these theories require the presence of density cavities, possibly auroral ionospheric cavities, or enhancements in the source region. The direct O/X mode maser theory [*Weatherwax et al.*, 1995; *Yoon et al.*, 1996] requires significant density cavities to provide a region for EM waves to reflect back and forth at the cavity walls, passing multiple times through the growth region within the cavity until they escape and are observed on the ground. Growth rate calculations predict that the X mode waves dominate [e.g., *Yoon et al.*, 1996], but recent observations of auroral roar polarization as the O mode [*Shepherd et al.*, 1997] make this an unlikely candidate for the generation of auroral roar emissions. More recent growth rate calculations by *Yoon et al.* [1998a] confirm previous calculations of a positive growth rate for the upper hybrid (UH) or Z mode [e.g., *Kaufmann*, 1980] and show that the Z mode growth rate far exceeds that of the O or X mode for f_{pe}/f_{ce} near $\sqrt{3}$ and 3. The Z mode is trapped in the ionosphere and a mode conversion mechanism is required to produce escaping O mode radiation. One

Table 1. F Region Ionospheric Parameters Measured With ISR During Times of Auroral Roar Emissions

Date	$(N_e)_{ave}$[a]	ΔL[b]	L_{ave}[b]	L_{min}[b]	E region arc	AIC	Matching	ap
Aug. 3, 1995	15.85	23	899	215	maybe	no	some	6
Aug. 15, 1995	8.32	23	383	64	yes	yes	100%	18
Nov. 1, 1995	9.77	23	497	110	yes	maybe	100%	32
March 12, 1996	7.76	44–137	864	116	yes	yes	100%	9
March 29, 1996[c]	6.76	23	304	83	yes	yes	100%	9
April 9, 1997	14.45	36	729	73	no	no	near 100%	6

Average electron density ($(N_e)_{ave}$), spatial resolution of the ISR measurements at 275 km (ΔL), average gradient scale length ($L_{ave} = |\nabla N_e/N_e|^{-1}_{ave}$), minimum gradient scale length ($L_{min} = |\nabla N_e/N_e|^{-1}_{min}$), presence of an E region arc, presence of an auroral ionospheric cavity (AIC), percent of altitude range over which the upper hybrid matching condition is observed, and 3-hourly ap index.

[a]Values are $\times 10^4$ cm^{-3}.

[b]Units are kilometers.

[c]Numbers are for a single radar scan.

such conversion mechanism is the Ellis Window which requires an inhomogeneous electron density in order for the Z mode waves to refract and achieve the conditions required for conversion (P. H. Yoon et al., Propagation of auroral radio waves to the ground, submitted to *Journal of Geophysical Research*, 1998). Another conversion mechanism requires a density cavity for growth of the fundamental Z mode waves and to provide reflection at the cavity walls for coalescence of Z mode waves into an escaping EM mode [*Willes et al.*, 1998]. The escaping radiation must be in the O mode for this theory to still be considered a candidate.

The typical auroral ionospheric cavities observed in Plates 2, 4, and 5 are ~50–70 km in latitudinal extent, are ~45–65% depleted relative to ambient densities, and appear to be adequate for the requirements of these theories. The presence of an ionospheric cavity also implies that horizontal gradients in the F region ionosphere also exist and could possibly be the location of wave mode conversion. It is tempting to conclude that these clear cases of ionospheric cavities, present during the simultaneous observation of auroral roar, support one of the previously mentioned theories. There is, however, one case that shows no signs of cavities. For this laminar case (Plate 1), it is unlikely that the spatial coverage of the instrument might simply fail to coincide with the source region since a laminar F region persists for many scans, and presumably the source region would eventually move through the path of the radar scanning magnetically North/South. Another possible scenario is that the temporal resolution (~5 min scan^{-1}) is too slow or the spatial resolution (~23 km) too large to capture a dynamic source region. In many of the events, auroral roar can be seen to change on a timescale of several seconds and high time resolution measurements show auroral roar is often composed of many narrow filaments that persist for only a few milliseconds and possibly less [*Shepherd et al.*, 1998].

Significant horizontal F region gradients appear in five of the six examples studied. Such gradients are an intrinsic feature of the source region in the Z mode Ellis window theory [*Yoon et al.*, 1998a], the Z mode coalescence theory [*Willes et al.*, 1998], and other theories for the mode conversion portion of an indirect generation mechanism including scattering on small-scale (5%) density fluctuations [*Bell and Ngo*, 1990] and wave-wave interactions [e.g., *Weatherwax et al.*, 1995]. Measured gradient scale lengths are summarized in Table 1. In order to characterize these gradients, we used the ISR density profiles from individual radar scans to compute normalized horizontal gradient scale lengths ($|\nabla N_e/N_e|^{-1}$) at six selected F region altitudes: 250, 260, 270, 280, 290, and 300 km. The spatial resolution of the data is the limiting scale of the ISR measurements at these altitudes, which varies from ~23 to 137 km and is summarized in Table 1. Both the maximum and average of the rectified and normalized gradient scale lengths over the entire horizontal range of the ISR scans are given in Table 1. The latter indicates an average value for the detectable F region electron density gradients, while the former measures the magnitude of the largest detected gradient. Table 1 illustrates the laminar nature of the August 3 event. The minimum normalized gradient scale length for this event is large (215 km) compared to the other events indicating that no significant horizontal gradients are present. Of course, no information is available about possible features during this event with scales less than ~30 km, which are probably also present in the F region ionosphere during auroral roar emissions and could be significant to their generation.

Auroral roar may be much more common in the ionosphere than it is at ground level [e.g., *Weatherwax et al.*, 1995]. The canonical explanation is that auroral arcs are most likely responsible for generating the emissions, but when they move directly overhead a ground station, they also screen the emissions from the ground due to the increased ionization raising the plasma frequency cutoff in the E region above the emission frequency. Conversely, the observed presence of auroral ionospheric cavities may serve to locally reduce the plasma frequency and allow HF ducting from the ionosphere to the ground. Plate 5 shows a sequence of ISR scans which support the screening hypothesis. The early scans (A through C) show a somewhat structured F region developing. Observation of auroral roar occurs primarily in segment C. An E region arc develops in scan A at 2318:13 UT, strengthens, and moves overhead in scan D near 2345:14 UT just at the termination of the auroral roar observation. ISR data from the August 15, November 1, and March 12 events (some ISR scans not shown) suggest a similar effect.

2.2. Upper Hybrid Frequency Matching

As previously mentioned, polarization measurements of auroral roar emissions [*Shepherd et al.*, 1997] indicate that direct X mode mechanisms cannot produce auroral roar emissions and suggest that an indirect mechanism involving, for example, electrostatic upper hybrid Z mode waves, is more likely. Such a mechanism requires a conversion to escaping O mode waves in order to explain the ground-based observations. Theoretical support for Z mode generation is given by *Kaufmann* [1980], who calculates that positive slopes in measured energetic electron distribution functions during rocket flights over bright aurora are large enough to drive electrostatic instabilities that peak when $f_{uh} = 2f_{ce}$. The role of UH waves is also supported by rocket data which show that UH waves are particularly intense when the condition $f_{uh} \approx 2f_{ce}$ is met [*Cartwright and Kellogg*, 1974; *Carlson et al.*, 1977]. For example, *Gough and Urban* [1983] observed strong modulations in the auroral electrons at the local upper hybrid frequency when $f_{uh} \sim 2.65$ MHz $\sim 2f_{ce}$. Recently, a more general electromagnetic treatment of the magnetoionic growth rate calculations confirms that the $Z2$ and $Z3$ modes are

largest when the upper hybrid matching condition is satisfied [*Yoon et al.*, 1998]. Here $Z2$ and $Z3$ represent Z mode waves at $2f_{ce}$ and $3f_{ce}$ respectively.

This Z mode generation theory requires that the upper hybrid matching condition be satisfied somewhere in the ionosphere at all the altitudes where the observed emission frequency matches the local gyroharmonic (2 or $3f_{ce}$). The ISR data can be used to test this mechanism as follows: first, the International Geomagnetic Reference Field (IGRF) model for the Earth's magnetic field [*International Association of Geomagnetism and Aeronomy Division I Working Group 1*, 1985] is used to determine the altitude profile of f_{ce}, $2f_{ce}$, and $3f_{ce}$. Second, the f_{ce} profile is combined with N_e measured by the ISR to obtain a profile of the upper hybrid frequency ($f_{uh}^2 = f_{ce}^2 + f_{pe}^2$) over the plane scanned by the radar. The upper hybrid matching condition ($f_{uh} = 2f_{ce}$ or $3f_{ce}$) is then determined over this plane. Finally, the observed auroral roar frequencies are used to compute an altitude range over which the matching condition must be satistfied. In Plates 1–6, a solid black contour on each color plot indicates where the computed upper hybrid matching condition $f_{uh} = 2f_{ce}$ or $3f_{ce}$ occurs based on the radar estimate of N_e, and a dotted and dashed contour indicate the larger region in which this condition may hold when the density-dependent uncertainty in the radar electron density measurement is taken into account. Horizontal dashed lines in each ISR scan mark the altitude range corresponding to the emission observed during the displayed scan. Likewise, the horizontal dotted lines represent the altitude range of the entire auroral roar event, including portions occurring before and after the radar scan shown. In order for the upper hybrid matching condition theory to explain the observed auroral roar emissions, a solid, dotted, or dashed contour must span the entire altitude range defined by the horizontal dashed lines.

Plate 1 shows that during the first roar event on August 3, 1995, the upper hybrid matching condition is not obtained in the F region during the observation of either $2f_{ce}$ or $3f_{ce}$ auroral emissions. For the time during which roar is observed at $3f_{ce}$ in segment B, a small region which satisfies the matching condition is seen around 300 km altitude, but none exists at higher altitudes to explain the lower frequencies of the observed emissions. Possible weak $3f_{ce}$ roar is observed in segment C with even less evidence of the matching condition. The time during which $2f_{ce}$ is most strongly observed in segment E shows essentially no upper hybrid matching in the required altitude range, except at the very lower edge (~200 km).

On the other hand, Plate 2 shows that on August 15, 1995, during the times of the strongest $2f_{ce}$ observation in segment D there is a region roughly 150 km geographically southeast of the radar where the matching condition is satisfied through the entire frequency range of the observed auroral emission. The matching condition also holds through the entire frequency ranges of less intense observed roar during segments B–E. Unfortunately there is limited radar data available for the time from 0301:08 to 0305:43 UT (panel F) during which an intense auroral roar is observed. However, even with the limited data it can be seen that matching exists nearly through the entire range of roar frequencies observed.

Plate 3 shows that often several spatially separated regions exist in the ionosphere for which the matching condition is satisfied over the observed frequency range of the emission. On November 1, 1995, starting at 1923:52 UT (segment A), regions approximately 100 km south, 100 km southwest, and 250 km northwest of the radar all show large areas where matching exists at all observed frequencies. In segments A–C, an area ~250 km long, 100-200 km southeast of the radar, in which the matching condition is satisfied through the entire observed emission frequency range, persists for nearly 20 min. Even during times of weak or intermittent roar emissions, such as segments D, E, and F, the matching condition occurs throughout nearly the observed auroral roar frequency range. As noted above, auroral roar may occur at these times in the ionosphere but is screened from the ground station by enhanced electron density at low altitudes.

Plate 4 shows auroral emissions on March 12, 1996, when the ISR performed a series of elevation scans. Strong emissions in segment A coincide with areas ~200 km southeast and ~300 km northwest of the radar where the matching condition is satisfied throughout the entire frequency range of the emission. In the subsequent radar scans B–D the matching condition exists at all observed roar frequencies, although the emission is weak or absent. The strong emission during segment E is most likely associated with a matching condition region nearly directly overhead.

Plate 5 shows a $2f_{ce}$ roar event on March 29, 1996 (segment C). Unfortunately, the fits to ISR autocorrelation functions exhibited large uncertainties above 300 km due to poor signal-to-noise ratio. Within these uncertainties, the matching condition appears to explain the full range of observed auroral roar frequencies. Similar regions where the matching condition is met occur in the other scans. In particular, the ISR briefly obtains data from >300 km in scan B which indicate that the matching condition exists at altitudes >300 km and probably throughout the full range of observed frequencies for this event.

Plate 6 shows that during the onset of the $2f_{ce}$ roar emission in segments A and B on April 9, 1997, the matching condition occurs through the entire frequency range of the observed auroral roar emission. During radar scan C, it appears probable that the matching condition is obtained over the entire range of auroral roar source altitudes, although this cannot be established with certainty due to large uncertainty in the radar measurements at critical locations. In scans D,

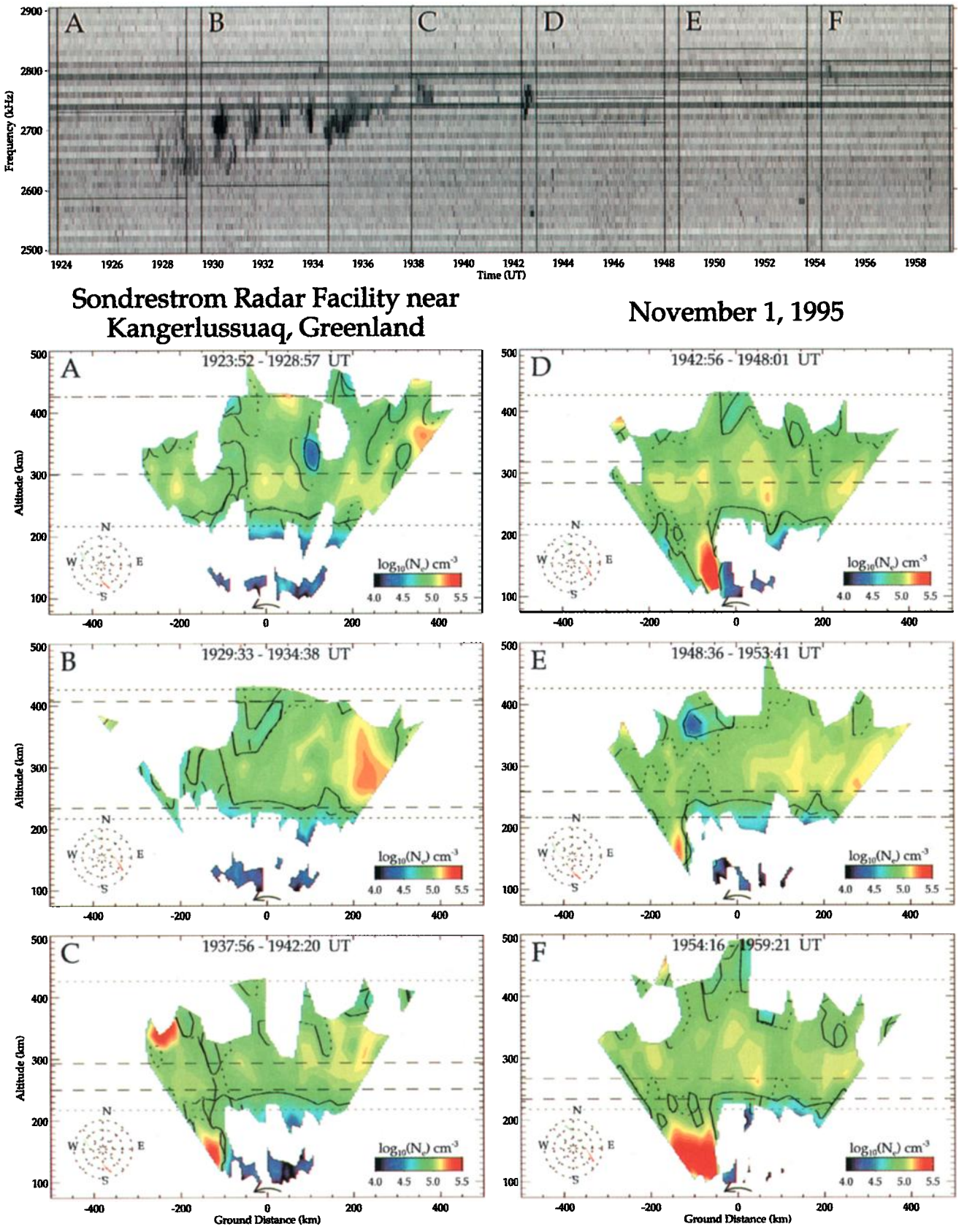

Plate 3. November 1, 1995. An example showing an E region arc, strong N_e gradients, and upper hybrid matching. A cavity-like density depletion is seen in Plate 3c immediately poleward of the E region arc.

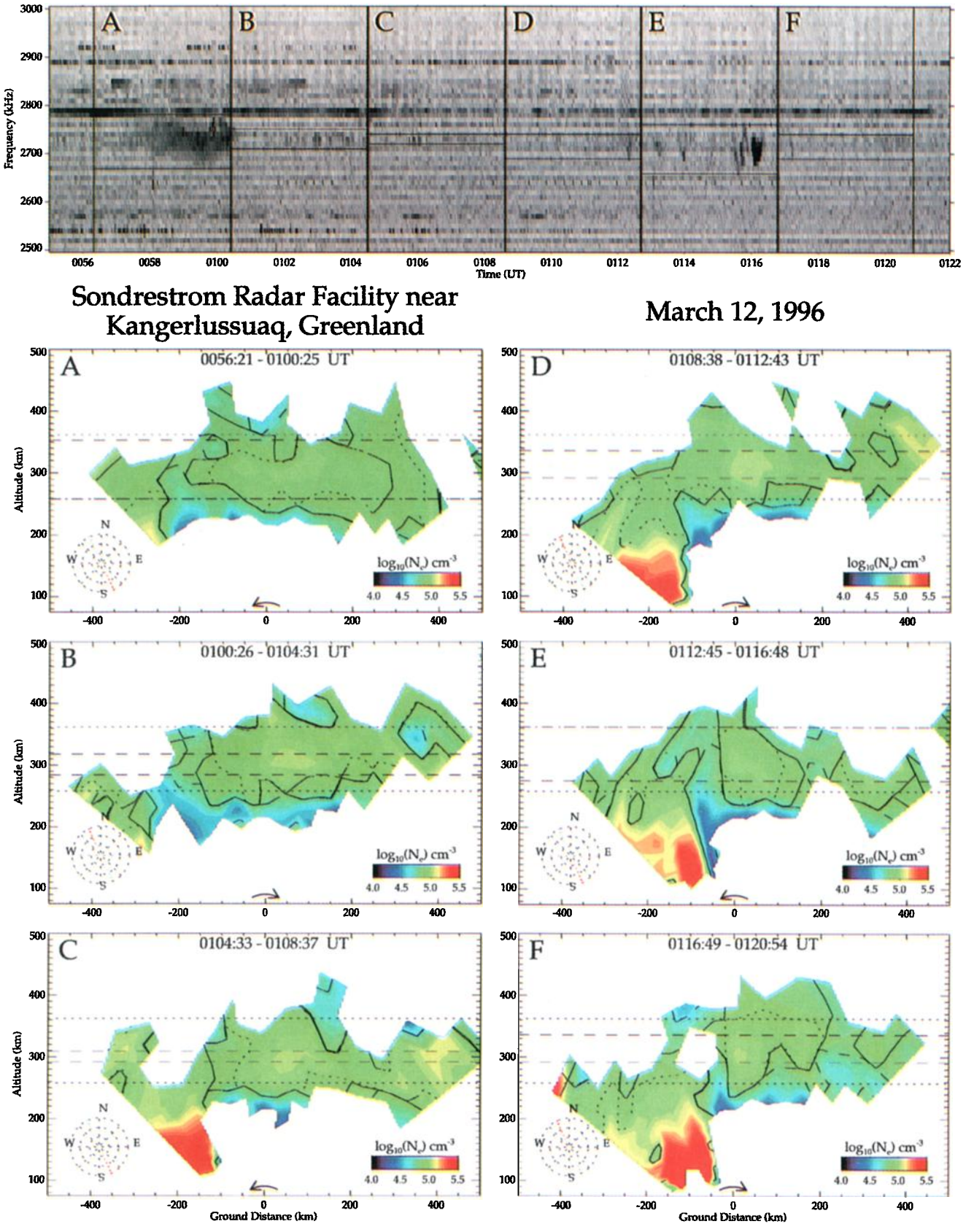

Plate 4. March 12, 1996. Elevation scans showing an E region arc, corresponding poleward auroral ionospheric cavity, strong N_e gradients, and regions of upper hybrid matching through the entire frequency range of the observed auroral roar emission.

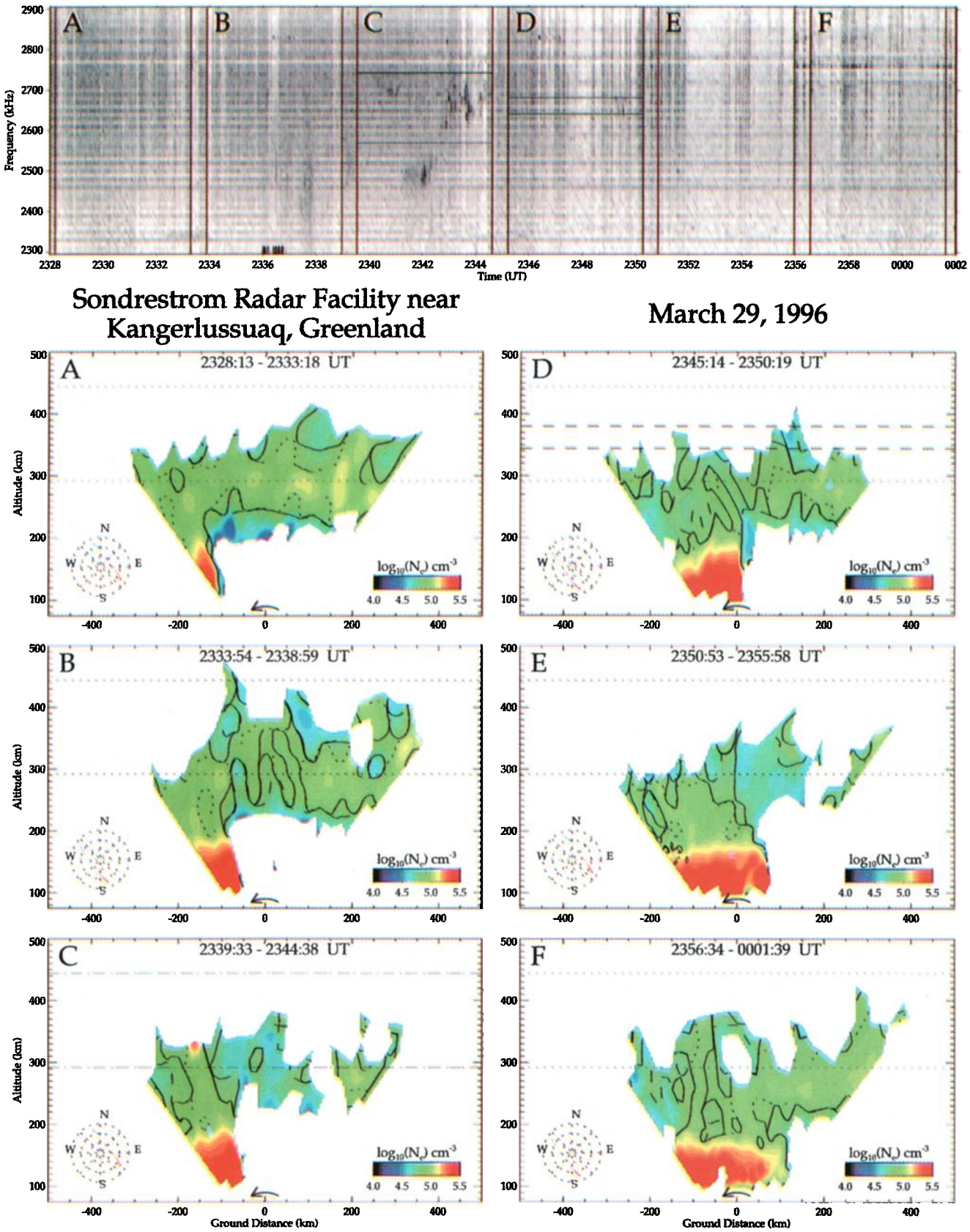

Plate 5. March 29, 1996. Another example, similar to Plate 2 with and E region arc, corresponding poleward auroral ionospheric cavity, strong N_e gradients, and upper hybrid matching. The latter scans show the screening of the source region by the E region arc.

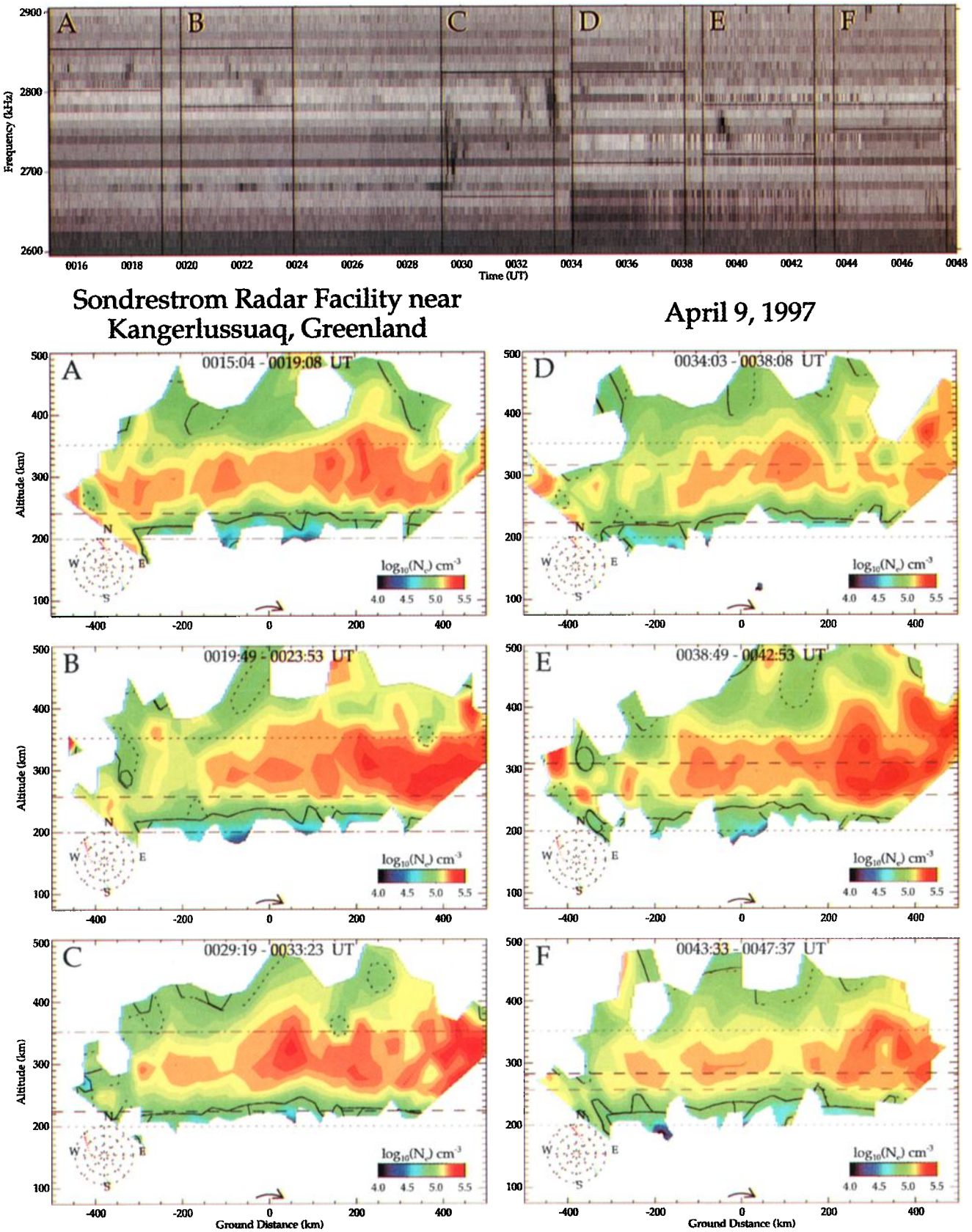

Plate 6. April 9, 1997. An example similar to Plate 1 in average N_e but with strong N_e gradients, and some regions where the upper hybrid matching condition is satisfied.

E, and F the matching condition is obtained 400 km south of the radar for a large part of the observed frequency range of weak intermittent roar emissions.

Table 1 summarizes the presence or absence of the hybrid matching condition $f_{uh} = 2f_{ce}$ or $3f_{ce}$ during the six days of auroral roar observations analyzed in this paper. The matching condition was satisfied at some location for nearly the entire frequency range of the observed auroral roar emissions in 16 out of 18 ISR scans. The matching condition was satisfied at least at some of the observed auroral roar frequency ranges for the remaining two cases. In particular, in all three elevation scans, in which the radar measures electron densities directly above the station, the upper hybrid matching condition is satisfied for the entire frequency range of the observed auroral roar emissions. These data strongly suggest that the upper hybrid matching condition plays a role in the generation of auroral roar. The few scans that have no matching between observed auroral roar frequency ranges could be attributed to the limited spatial/temporal resolution and spatial coverage of the ISR as configured for these runs. As previously stated, radio data from other stations suggest that auroral roar most likely originate from nearly overhead, and add greater weight to the three elevation scans which all show matching regions (see Plate 4). At the very least, the ISR data do not rule out the theories of auroral roar generation which are based on excitation of upper hybrid waves when $f_{uh} = 2f_{ce}$ or $3f_{ce}$.

3. Conclusions

Characterization of the structure of the ionosphere during auroral roar observations is critical as the proposed generation mechanisms all rely on the presence of structure and/or gradients in the electron density at F region altitudes. Several theories rely on density cavities, such as auroral ionospheric cavities, to enhance wave growth by reflecting the waves multiple times through a source region, to provide for conversion of trapped Z mode waves to escaping O mode radiation, or to duct O or X mode radiation. Other generation mechanisms rely on theory that predicts excitation of upper hybrid Z mode waves where $f_{uh} = 2f_{ce}$ or $3f_{ce}$, a condition that can be tested using density profiles obtained from the Sondrestrom ISR.

The ISR data show that no particular density feature persists in all the cases for which auroral roar emissions are observed, at least at scale sizes $>\sim$30 km probed by the radar. Table 1 summarizes the results. Five of the six cases show strong electron density gradients, and three (possibly four) of these events are characterized by the observation of an auroral ionospheric cavity. One case has no apparent density structure and remains laminar during the auroral roar observations. It is possible that the spatial/temporal resolution and spatial coverage of the ISR, as configured for these particular runs, was simply too limited to address density features critical to the evaluation of cavity theories. In five of six cases, $|\nabla N_e/N_e|^{-1}_{min} < 120$ km (measured with 23–137 km resolution). An auroral roar radiowave imager, planned for installation at the Sondrestrom site in the Summer of 1998, will be used to identify the location of the source region and narrow the ISR beam coverage, minimizing the possibility of missing the source region.

In 16 of 18 radar scans on 5 of the 6 days studied the upper hybrid matching condition $f_{uh} = 2f_{ce}$ or $3f_{ce}$ is satisfied in the F region ionosphere over nearly the entire frequency range of the observed $2f_{ce}$ or $3f_{ce}$ auroral roar emissions. The few cases in which the matching condition is not observed may result because the radar does not sample the entire ionosphere and has limited spatial and temporal resolution as configured for other experiments. These data are consistent with a theory of auroral roar in which an electrostatic upper hybrid or Z mode wave is generated at F region altitudes and subsequently mode converts to an escaping EM wave which propagates to the ground.

Acknowledgments. This research was supported by National Science Foundation grants ATM-9713119 to Dartmouth College and ATM-9616136 to the University of Maryland. The authors would like to thank Mike Trimpi for his work in designing, building, and deploying the Dartmouth College radio receiver, and John and Tommy Jørgensen for their help maintaining and operating this receiver. Operation of the Sondrestrom ISR and support for analysis of ISR products was provided by NSF cooperative agreement ATM-9317167.

The Editor thanks J. Minow and another referee for their assistance in evaluating this paper.

References

Bell, T. F., and H. D. Ngo, Electrostatic lower hybrid waves excited by electromagnetic whistler mode waves scattering from planar magnetic-field-aligned plasma density irregularities, *J. Geophys. Res.*, *95*, 149, 1990.

Carlson, C. W., R. E. Ergun, and M. K. Hudson, Observations of beam generated upperhybrid waves parametrically decaying into whistlers, *Eos Trans. AGU*, *58*, 1214, 1977.

Cartwright, D. E., and P. J. Kellogg, Observations of radiation from an electron beam artificially injected into the ionosphere, *J. Geophys. Res.*, *79*, 1439, 1974.

Doe, R. A., M. Mendillo, J. F. Vickrey, L. J. Zanetti, and R. W. Eastes, Observations of nightside auroral cavities, *J. Geophys. Res.*, *98*, 293, 1993.

Gough, M. P., and A. Urban, Auroral beam/plasma interaction observed directly, *Planet. Space Sci.*, *31*, 875, 1983.

Hughes, J. M., and J. LaBelle, The latitude dependence of auroral roar, *J. Geophys. Res.*, *103*, 14911, 1998.

International Association of Geomagnetism and Aeronomy Division I Working Group 1, International geomagnetic reference field: Revision 1985, *J. Geomagn. Geoelectr.*, *37*, 1157, 1985.

Kaufmann, R. L., Electrostatic wave growth: Secondary peaks in a measured auroral electron distribution function, *J. Geophys. Res.*, *85*, 1713, 1980.

Kellogg, P. J., and S. J. Monson, Radio emissions from the aurora, *Geophys. Res. Lett.*, *6*, 297, 1979.

Kellogg, P. J., and S. J. Monson, Further studies of auroral roar, *Radio Sci.*, *19*, 551, 1984.

Kelly, J. D., C. J. Heinselman, J. F. Vickrey, and R. R. Vondrak, The Sondrestrom radar and accompanying ground-based instrumentation, *Space Sci. Rev.*, *71*, 797, 1995.

LaBelle, J., and A. T. Weatherwax, Ground-based observations of LF/MF/HF radio waves of auroral origin, in *Physics of Space Plasmas (1992)*, edited by T. Chang, p. 223, Scientific, Cambridge, Mass., 1992.

LaBelle, J., M. L. Trimpi, R. Brittain, and A. T. Weatherwax, Fine structure of auroal roar emissions, *J. Geophys. Res.*, *100*, 21,953, 1995.

LaBelle, J., S. G. Shepherd, and M. L. Trimpi, Observations of auroral medium frequency bursts, *J. Geophys. Res.*, *102*, 22221, 1997.

Shepherd, S. G., J. LaBelle, and M. L. Trimpi, The polarization of auroral radio emissions, *Geophys. Res. Lett.*, *24*, 3161, 1997.

Shepherd, S. G., J. LaBelle, and M. L. Trimpi, Further investigation of auroral roar fine structure, *J. Geophys. Res.*, *103*, 2219, 1998.

Weatherwax, A. T., Ground-based observations of auroral radio emissions, Ph.D. thesis, Dartmouth Coll., Hanover, N. H., 1994.

Weatherwax, A. T., J. LaBelle, M. L. Trimpi, and R. Brittain, Ground-based observations of radio emissions near $2f_{ce}$ and $3f_{ce}$ in the auroral zone, *Geophys. Res. Lett.*, *20*, 1447, 1993.

Weatherwax, A. T., J. LaBelle, and M. L. Trimpi, A new type of auroral radio emission observed at medium frequencies (~1350-3700 kHz) using ground-based receivers, *Geophys. Res. Lett.*, *21*, 2753, 1994.

Weatherwax, A. T., J. LaBelle, M. L. Trimpi, R. A. Treumann, J. Minow, and C. Deehr, Statistical and case studies of radio emissions observed near $2f_{ce}$ and $3f_{ce}$ in the auroral zone, *J. Geophys. Res.*, *100*, 7745, 1995.

Weber, E. J., J. F. Vickrey, H. Gallagher, L. Weiss, C. J. Heinselman, R. A. Heelis, and M. C. Kelley, Coordinated radar and optical measurements of stable auroral arcs at the polar cap boundary, *J. Geophys. Res.*, *96*, 17,847, 1991.

Willes, A. J., S. D. Bale, and Z. Kuncic, A z mode electron-cyclotron maser model for bottomside ionospheric harmonic radio emissions, *J. Geophys. Res.*, *103*, 7017, 1998.

Yoon, P. H., A. T. Weatherwax, T. J. Rosenberg, and J. LaBelle, Lower ionospheric cyclotron maser theory: A possible source of $2f_{ce}$ and $3f_{ce}$ auroral radio emissions, *J. Geophys. Res.*, *101*, 27,015, 1996.

Yoon, P. H., A. T. Weatherwax, and T. J. Rosenberg, On the generation of auroral radio emissions at harmonics of the lower ionospheric electron cyclotron frequency: X, O, and Z mode maser calculations, *J. Geophys. Res.*, *103*, 4071, 1998.

R. A. Doe and M. McCready, Radio Science and Engineering Division, SRI International, 333 Ravenswood Avenue, Menlo Park, CA 94025. (doe@unix.sri.com; mccready @chaos.sri.com)

J. LaBelle and S. G. Shepherd, Department of Physics and Astronomy, Dartmouth College, Wilder Hall, Hinmann Box 6127, Hanover, NH 03755. (jlabelle@einstein.dartmouth.edu; simon@newton.dartmouth.edu)

A. T. Weatherwax, Institute for Physical Science and Technology, University of Maryland, College Park, MD 20742. (allanw@polar.umd.edu)

(Received April 24, 1998; revised July 1, 1998;
accepted July 1, 1998.)